LIVERPOOL JOHN MOORES UNIVERSITY

LJMU Research Online

Teipel, S, Dyrba, M, Ballarini, T, Brosseron, F, Bruno, D, Buerger, K, Cosma, N-C, Dechent, P, Dobisch, L, Duzel, E, Ewers, M, Fliessbach, K, Haynes, JD, Janowitz, D, Kilimann, I, Laske, C, Maier, F, Metzger, CD, Munk, MH, Peters, O, Pomara, N, Preis, L, Priller, J, Ramirez, A, Roy, N, Scheffler, K, Schneider, A, Schott, BH, Spottke, A, Spruth, EJ, Wagner, M, Wiltfang, J, Jessen, F and Heneka, M

Association of cholinergic basal forebrain volume and functional connectivity with markers of inflammatory response in the Alzheimer's disease spectrum

http://researchonline.ljmu.ac.uk/id/eprint/15939/

Article

Citation (please note it is advisable to refer to the publisher's version if you intend to cite from this work)

Teipel, S, Dyrba, M, Ballarini, T, Brosseron, F, Bruno, D, Buerger, K, Cosma, N-C, Dechent, P, Dobisch, L, Duzel, E, Ewers, M, Fliessbach, K, Haynes, JD, Janowitz, D, Kilimann, I, Laske, C, Maier, F, Metzger, CD, Munk, MH, Peters, O. Pomara. N. Preis. L. Priller. J. Ramirez. A. Rov. N. Scheffler. K. Schneider.

LJMU has developed **LJMU Research Online** for users to access the research output of the University more effectively. Copyright © and Moral Rights for the papers on this site are retained by the individual authors and/or other copyright owners. Users may download and/or print one copy of any article(s) in LJMU Research Online to facilitate their private study or for non-commercial research. You may not engage in further distribution of the material or use it for any profit-making activities or any commercial gain.

The version presented here may differ from the published version or from the version of the record. Please see the repository URL above for details on accessing the published version and note that access may require a subscription.

http://researchonline.ljmu.ac.uk/

For more information please contact researchonline@ljmu.ac.uk

http://researchonline.ljmu.ac.uk/

Association of cholinergic basal forebrain volume and functional connectivity with markers of inflammatory response in the Alzheimer's disease spectrum

Stefan J. Teipel[1,2], Martin Dyrba[1], Tommaso Ballarini[3], Frederic Brosseron[3,4], Davide Bruno[5], Katharina Buerger[6,7], Nicoleta-Carmen Cosma[8], Peter Dechent[9], Laura Dobisch[10], Emrah Düzel[10,11], Michael Ewers[6,7], Klaus Fliessbach[3,4], John D. Haynes[12], Daniel Janowitz[7], Ingo Kilimann[1,2], Christoph Laske[13,14,15], Franziska Maier[16], Coraline D. Metzger[10,11,17], Matthias H. Munk[13,14,15], Oliver Peters[8,18], Nunzio Pomara[19,20], Lukas Preis[8], Josef Priller[18,21,22], Alfredo Ramírez[3,4,16], Nina Roy[3], Klaus Scheffler[23], Anja Schneider[3,4], Björn H. Schott[24,25,26], Annika Spottke[3,27], Eike J. Spruth[18,21], Michael Wagner[3,4], Jens Wiltfang[24,25,28], Frank Jessen[3,16,29], Michael T. Heneka[3,4]

[1] German Center for Neurodegenerative Diseases (DZNE), Rostock, Germany
[2] Department of Psychosomatic Medicine, University of Rostock, Rostock, Germany
[3] German Center for Neurodegenerative Diseases (DZNE), Bonn, Germany
[4] Department for Neurodegenerative Diseases and Geriatric Psychiatry, University Hospital Bonn, Bonn, Germany
[5] School of Psychology, Liverpool John Moores University, Liverpool, UK
[6] German Center for Neurodegenerative Diseases (DZNE), Munich, Germany
[7] Institute for Stroke and Dementia Research (ISD), University Hospital, Ludwig Maximilian University, Munich, Germany
[8] Department of Psychiatry and Psychotherapy, Charité – Universitätsmedizin Berlin, Campus Benjamin Franklin, Berlin, Germany
[9] MR-Research in Neurosciences, Georg-August-University, Goettingen, Germany
[10] German Center for Neurodegenerative Diseases (DZNE), Magdeburg, Germany
[11] Institute of Cognitive Neurology and Dementia Research (IKND), Otto-von-Guericke University, Magdeburg, Germany
[12] Bernstein Center for Computational Neuroscience, Berlin, Germany
[13] German Center for Neurodegenerative Diseases (DZNE), Tuebingen, Germany
[14] Section for Dementia Research, Hertie Institute for Clinical Brain Research, Tuebingen, Germany
[15] Department of Psychiatry and Psychotherapy, University of Tuebingen, Tuebingen, Germany
[16] Department of Psychiatry, Medical Faculty, University of Cologne, Cologne, Germany
[17] Department of Psychiatry and Psychotherapy, Otto-von-Guericke University, Magdeburg, Germany
[18] German Center for Neurodegenerative Diseases (DZNE), Berlin, Germany
[19] Nathan Kline Institute for Psychiatric Research, Orangeburg, NY, USA
[20] Department of Psychiatry, School of Medicine, New York University, New York City, NY, USA
[21] Department of Psychiatry and Psychotherapy, Charité – Universitätsmedizin Berlin, Campus Charité Mitte, Berlin, Germany
[22] Department of Psychiatry and Psychotherapy, Klinikum rechts der Isar, Technical University Munich, Munich
[23] Department for Biomedical Magnetic Resonance, University of Tuebingen, Tuebingen, Germany
[24] German Center for Neurodegenerative Diseases (DZNE), Goettingen, Germany
[25] Department of Psychiatry and Psychotherapy, University Medical Center Goettingen, Goettingen, Germany
[26] Leibniz Institute for Neurobiology, Magdeburg, Germany
[27] Department of Neurology, University Hospital Bonn, Bonn

[28] Neurosciences and Signaling Group, Institute of Biomedicine (iBiMED), Department of Medical Sciences, University of Aveiro, Aveiro, Portugal
[29] Excellence Cluster on Cellular Stress Responses in Aging-Associated Diseases (CECAD), University of Cologne, Cologne, Germany

Running Title: Cholinergic basal forebrain and inflammation

Manuscript requirements:

Title:	151
Abstract:	244
Text:	5310
References:	63
Tables	1
Figures	5
Supplementary Tables	1
Supplementary Figures	6

Corresponding Author:
Stefan J. Teipel, M.D.
Department of Psychosomatic Medicine
University of Rostock,
and DZNE Rostock,
Gehlsheimer Str. 20,
18147 Rostock, Germany
Tel.: 01149-381-494-9470
Fax: 01149-381-494-9472
E-mail: stefan.teipel@med.uni-rostock.de

Abstract

Background: Inflammation has been described as a key pathogenic event In Alzheimer's disease (AD), downstream of amyloid and tau pathology. Preclinical and clinical data suggest that the cholinergic basal forebrain may moderate inflammatory response to different pathologies.

Objective: To study the association of cholinergic basal forebrain volume and functional connectivity with measures of neuroinflammation in people from the AD spectrum

Methods: We studied 261 cases from the DELCODE cohort, including people with subjective cognitive decline, mild cognitive impairment, AD dementia, first degree relatives and healthy controls. Using Bayesian ANCOVA, we tested associations of MRI indices of cholinergic basal forebrain volume and functional connectivity with CSF levels of sTREM2 as a marker of microglia activation, and serum levels of complement C3. Using Bayesian elastic net regression, we determined associations between basal forebrain measures and a large inflammation marker panel from CSF and serum.

Results: We found anecdotal to moderate evidence in favor of the absence of an effect of basal forebrain volume and functional connectivity on CSF sTREM2 and serum C3 levels both in Aβ42/ptau-positive and negative cases. Bayesian elastic net regression identified several CSF and serum markers of inflammation that were associated with basal forebrain volume and functional connectivity. The effect sizes were moderate to small.

Conclusion: Our data-driven analyses generate the hypothesis that cholinergic basal forebrain may be involved in the neuroinflammation response to Aβ42 and phospho-tau pathology in people from the AD spectrum. This hypothesis needs to be tested in independent samples.

Key words: neuroinflammation; cholinergic system; Alzheimer's disease; MRI; CSF; plasma; sTREM2

Introduction

Alzheimer's disease (AD) is characterized by a complex interplay of upstream pathologies, such as cerebral amyloid accumulation, and downstream effects on neuronal structural and functional integrity, partly mediated by neuroinflammatory response [1-3]. Interestingly, these effects seem to work in both directions. Thus, changes in neuronal functional activity and inflammation result from abnormal amyloid accumulation [4, 5]. At the same time, microglia derived neuroinflammatory factors can facilitate or even induce Aβ production [6, 7].

The cholinergic system is affected early in AD [8], and it is believed to moderate the inflammatory response to different pathologies [9]. Selective stimulation or suppression of basal forebrain cholinergic neuron activity in mice affected the peripheral expression of TNFalpha levels in response to endotoxemia [10]. This finding indicated that central action of acetylcholine on muscarinic acetylcholine receptors in the brain may suppress circulating TNFalpha and other proinflammatory cytokines. Similarly, the centrally acting acetylcholinesterase inhibitor galantamine suppressed an acid aspiration-induced acute respiratory syndrome in rabbits [11]. Consistent with the suspected association of cholinergic system integrity with inflammatory response, higher baseline expression of complement C3 in blood and a larger longitudinal increase of soluble TREM2 (sTREM2) levels in the CSF were associated with higher rates of atrophy of basal forebrain volume in cognitively healthy people with an increased CSF tau to amyloid ratio [12]. These effects were interpreted to indicate microglia involvement into clearance of amyloid and tau and resulting inflammatory responses. Taken together with the preclinical data on a modulatory role of cholinergic activity [10, 11], these data suggest that loss of structural integrity of the cholinergic basal forebrain may unleash the microglial inflammatory response to amyloid and tau accumulation.

Here, we leveraged structural and resting state functional MRI, CSF and blood data from the DELCODE cohort [13] to extend these previous findings to the AD spectrum. First, in a hypothesis-driven approach we determined the effect of basal forebrain volume [14, 15] on levels of sTREM2 in the CSF and complement C3 in serum, controlling for Aβ and ptau status as well as clinical diagnosis across the AD spectrum. Secondly, extending previous evidence we determined associations between sTREM2 and complement factor C3 with resting state functional connectivity of the basal forebrain [16, 17]. Thirdly, we determined the association of a broad neuroinflammatory marker panel in CSF and serum with basal forebrain volume and functional connectivity. For this data-driven analysis we chose a Bayesian approach with an elastic net penalty [18] to directly estimate the plausibility of the presence or absence of an effect and its strength, and to avoid overfitting in the presence of large number of predictors. The data of these analyses can serve a better understanding of the possible role of cholinergic basal forebrain in the central and peripheral inflammatory response to Aβ and tau pathology in the AD spectrum.

Material and Methods

Participants

We used the baseline data, including n = 1,079 participants, of the multicenter DELCODE study, conducted by the German Center for Neurodegenerative Diseases (DZNE) [13]. We excluded cases without available CSF inflammatory biomarkers, leaving 309 cases. After removing cases without an available MRI scan, we included 261 cases for further analysis. The sample group consisted of older healthy controls, first-degree relatives of a person with a documented diagnosis of AD dementia, and participants with AD, MCI or subjective cognitive decline (Table 1). DELCODE excluded participants with a current major depressive episode, past or present major psychiatric disorders, neurological diseases other than AD, or unstable medical condition [13]. Subjective cognitive decline (SCD) was defined as a persistent self-perceived cognitive decline in the absence of objective cognitive impairment as measured by the CERAD test battery, lasting at least for 6 months and being unrelated to an acute event [19]. The MCI patients met the core clinical criteria for MCI according to National Institute on Aging-Alzheimer's Association (NIA-AA) workgroup guidelines [20]. The AD patients had a clinical diagnosis of probable AD dementia according to the NIA-AA workgroups guidelines [21]. The control participants had no objective cognitive impairment in cognitive tests, no history of neurological or psychiatric disease and did not report self-perceived cognitive decline. All participants or their representatives provided written informed consent. The study protocol was approved by the local institutional review boards and ethical committees of the participating centers. It was conducted in accord with the Helsinki Declaration of 1975.

Biomaterial sampling and fluid biomarker acquisition

Biomaterial sampling procedures and biomarker measurements for DELCODE have been described elsewhere [13]. In brief, material is sampled by trained study personal following standard operating procedures (SOP) for collection and storage of samples. Both serum and CSF samples were aliquoted after centrifugation and stored at -80 °C until analysis.

Image acquisition

The data were acquired from nine Siemens 3.0 Tesla MRI scanners (4 Verio, 1 Skyra, 3 TimTrio and 1 Prisma system) using identical acquisition parameters and harmonized instructions. To ensure high image quality throughout the acquisition phase, all scans had to pass a semi-automated quality check during the study conduction, so that protocol deviations could be reported to the study sites, and the acquisition at the respective site could be adjusted. Functional MRI was based on a T2*-weighted echo-planar imaging (EPI) sequence using a 64×64 image matrix with 47 axial slices (thickness 3.5 mm, no gap) and interleaved acquisition. The field of view was 224×224×165 mm, isotropic voxel size of 3.5 mm, echo time 30 ms, repetition time 2,580 ms, flip angle 80◦, and parallel imaging acceleration factor 2. The sequence took 7 min 54 s. High-resolution T1-weighted anatomical images were obtained using a sagittal magnetization-prepared rapid gradient echo (MPRAGE) sequence (field of view 256 × 256 mm, matrix size 256 × 256, isotropic voxel size 1 mm, echo time 4.37 ms, flip angle 7°, repetition time 2500 ms, number of slices 192, parallel imaging acceleration factor 2). The duration of the sequence was 5 min 8 s.

CSF AD biomarker assessment

Biomarker data were provided by the DELCODE data management. AD markers had been determined using commercially available kits according to vendor specifications: V-PLEX Aβ Peptide Panel 1 (6E10) Kit (K15200E) and V-PLEX Human Total Tau Kit (K151LAE) (Mesoscale Diagnostics LLC, Rockville, USA), and Innotest Phospho-Tau(181P) (81581; Fujirebio Germany GmbH, Hannover, Germany). For amyloid and tau isoforms, cut-off values for amyloid / tau isoforms were based on Gaussian mixture modeling of the DELCODE data independent of any group assignments using the R package flexmix (version 2.3-15) [22]: Amyloid ratio (A) Aβ42/Aβ40 0.08; tau pathology (T) by p-tau-181 73.65 pg/ml; neurodegeneration (N) by t-tau 510.9 pg/ml. We calculated the Aβ42/ptau ratio for each participant to classify cases into AD pathology positive and negative cases, respectively.

CSF and serum inflammatory marker panel assessment

The inflammatory panel contained proteins with robust detection in both CSF and serum, related to inflammation and other mechanisms (ferritin, ApoE, sTrem2, sAXL, sTyro3, IL-6, IL-18, MCP-1, IP-10, MIF, YKL-40, CRP, complement factors C1q, C3, C3b, C4, factor B, factor H) as well as neurogranin and FABP-3 as non-tau related markers of neurodegeneration. Data of experimental biomarkers were provided by the DELCODE data management. In brief, all fluid biomarkers had been determined by use of commercially available enzyme-linked immunosorbent assays (ELISA) utilizing different assays formats and detection technologies optimized to the respective target's dilution factors, detection range and multiplexing options, as described in [23]. Assay performance was controlled by use of internal control samples, with data determined in duplicates with a maximum coefficient of variance (CV) of 20%.

Imaging data processing

The **T1-weighted anatomical images** were initially coregistered to the mean functional images and subsequently preprocessed using the Computational Anatomy Toolbox (CAT12, v9.6/r7487[24] for Statistical Parametric Mapping 12 (SPM12, v12.6/r1450, Wellcome Centre for Human Neuroimaging, London, UK). The images were segmented into grey matter (GM), white matter (WM) and CSF, followed by spatial normalization to the default CAT12 brain template in Montreal Neurological Institute (MNI) reference space using the Diffeomorphic Anatomical Registration Through Exponentiated Lie Algebra (DARTEL) algorithm. During this step, the images were resliced to an isotropic voxel size of 1.5 mm, and modulated to adjust for expansion and shrinkage of the grey matter tissue. We then applied a mask containing the cholinergic nuclei of the basal forebrain [14] to derive the raw basal forebrain volumes. The raw volumes were divided by the total intracranial volume to adjust for head size. The resulting normalized basal forebrain volumes were entered in the statistical models.

Functional MRI data processing was carried out using Data Processing Assistant for Resting-State fMRI Advanced (DPARSFA 4.3) [25]. After the removal of the first ten images, we applied a series of steps including slice timing correction and realignment to eliminate the head motion. Scans with excessive head motion, i.e., a framewise displacement of greater than 0.5 mm for more than 30 % of the scan duration, were excluded. We regressed out linear detrend, 24 head motion parameters, WM and CSF signal as nuisance regressors, to reduce the influence of noise. The functional images were band pass filtered to 0.1-0.01 Hz and spatially normalized to MNI space by applying the deformation fields estimated for the coregistered T1-weighted images beforehand. During warping, the functional images were resliced to an isotropic voxel resolution of 3 mm and finally smoothed with a 6 mm full-width-at-half-maximum (FWHM) Gaussian kernel. Based on the previous study [16], we defined the two functional subdivisions of the basal forebrain, anterior and posterior basal forebrain, as seeds

for the functional connectivity analyses. Global functional connectivity was determined based on Pearson correlation coefficient of the seed region's and all other GM voxel's time series [26]. The resulting voxel-wise functional connectivity maps were Fisher z-transformed, thresholded at $z \geq 0.3$ ($p < 0.001$) to define the respective functional connectivity networks, and averaged to produce the global functional connectivity values. Note that we included only positive correlation coefficients for computing the global connectivity, because positive and negative correlations otherwise may cancel each other out when averaging the correlation coefficients. Global connectivity values, one for each individual and functional division of the basal forebrain, were entered into the subsequent statistical analysis.

Statistical analysis

Statistical analyses were conducted in a Bayesian framework to allow estimation of model plausibility and determining effect sizes with credibility intervals. The analyses were conducted in two steps:

The first step was a hypothesis driven analysis of the effect of basal forebrain volumes on CSF TREM2 and serum complement C3, following previous evidence [12]. Consequently, we determined plausibility of regression models using CSF TREM2 or serum complement C3 as dependent variables, respectively, and basal forebrain volume as predictor with age, sex, education years and dummy-coded diagnosis as covariates, separately for Aβ42/ptau-positive and Aβ42/ptau-negative cases. These index models were compared with the null models only containing the covariates. We used *Bayes factor (BF) hypothesis testing* to compare the index models containing the marker of interest against the null model. This approach allowed us to accept the best possible hypothesis for the data [27, 28]. We used *Jeffreys' Amazing Statistics Program (*JASP Version 0.11), available at jasp-stats.org, to calculate the models. We report

the Bayes Factor (BF_{10}) quantifying evidence against the null hypotheses. To address potential issues with non-normally distributed residuals in the multiple regressions we applied Markov-Monte Carlo chain sampling to each analysis 1,000 times. We used the JASP default JZS prior. We decided a priori to follow up the size of the marker effect only for index models with at least moderate plausibility, i.e. $BF_{10} > 3$.

The *second step* was a data-driven candidate marker selection based on the 20 CSF and 20 serum inflammatory markers. Previous to the subsequent analyses all variables were scaled to zero mean and unit standard deviation.

Due to the large number of predictors and their expected collinearity we used regularized regression. Regularization aims to avoid overfitting of a model with a large number of predictors [29]. The penalty term used for regularization shrinks parameters towards zero and more so for small than large parameters [30], see supplementary Figure 4 for an example. The Bayesian framework offers a wide variety of shrinkage priors, such as lasso, elastic net, or ridge [31]. We chose an *elastic net* penalty term that provides a reasonable compromise between both ridge and lasso penalties [18, 32] and allows selecting groups of correlated features from a high number of candidate markers [18]. The full Bayesian approach, as implemented in the library "bayesreg" in R (accessed through R Studio, version 1.1.463), allows for simultaneous estimation of both penalty parameters and model parameters [30, 31]. We used one half of the data as training data to estimate the parameter weights and the other half as the test data to determine the parameter fit.

From the regularized regression models, we selected the most relevant parameters based on their credibility intervals. Thus, a parameter was kept in the model if its credibility interval did not contain zero, and was excluded otherwise. The *credibility interval* provides the probability that the population parameters lie between the particular upper and lower bounds [33]. The

credibility interval thresholds leading to most accurate feature selection with the Bayes elastic net have extensively been studied using simulations [30]. A credibility interval of 95% was found to be too wide, whereas a credibility interval of 50% was found to be most efficient in providing a set of variables with the highest fit of the true data [30]. Consequently, a credibility interval of 50% is the default in penalized regression in “bayesreg” or other libraries like “rstanarm”, and was used here as well.

Results

Demographic and basal forebrain between group differences

As shown in Table 1, participants were highly likely to differ in age, sex, and, as expected, in MMSE scores, but not in years of education across diagnostic groups.

We found extreme evidence for an effect of diagnosis on basal forebrain volume after controlling for age and sex, with a Bayes factor of $1.3*10^{32}$ in favor of an effect of diagnosis. Evidence was in favor of no effect of diagnosis for anterior and posterior basal forebrain division functional connectivity (BF_{10} = 0.065 and 0.132, respectively). Further details on the post hoc comparisons across diagnostic groups can be found in the supplementary material, including supplementary Table 1 and supplementary Figures 1, 2, and 3.

Basal forebrain volume and functional connectivity vs. CSF TREM2 and serum C3

Using Bayesian ANCOVA in JASP, we compared the null model, including age, sex, education years, and diagnosis, with the index models, additionally including the volume or functional connectivity measures as predictors.

In the **Aβ42/ptau-positive cases**, the model predicting **CSF-TREM2** by **basal forebrain volume** yielded a Bayes factor of 0.438, indicating that this model was 2.28 times less likely than the null model only containing the covariates. Similarly, **in the Aβ42/ptau-negative cases**, the model with basal forebrain volume was 4.0 times less likely than the null model (BF_{10} = 0.250).

In the **Aβ42/ptau-positive cases**, the model predicting **serum complement C3** by **basal forebrain volume** was 2.0 times less likely than the null model (BF_{10} = 0.498). In the **Aβ42/ptau-negative cases**, the serum complement C3 model was 3.0 times less likely than the null model (BF_{10} = 0.331).

In **17 amyloid positive SCD cases and controls**, similarly to the full sample analysis, we found anecdotal level of evidence in favor of the absence of an effect of Bf volume on CSF sTREM2 levels (BF_{01} = 1.9) and serum complement C3 (BF_{01} = 1.7).

When using **anterior and posterior basal forebrain functional connectivity** as predictor variables, respectively, none of the models showed more than anecdotal evidence for CSF TREM2 or serum complement C3 as dependent variables; in fact, most models showed anecdotal to moderate evidence in favor of the null model (data not shown).

Since we found no evidence in favor of the index models, we conducted no further follow-up effect size estimates.

A complementary Bayesian implementation of robust regression, an approach, which is less sensitive to outliers than classical ANCOVA models, yielded no evidence for relevant effects of BF volume on CSF sTREM2 and serum complement C3 levels as well (see Supplementary analysis).

Basal forebrain volume and connectivity and central and peripheral inflammatory markers

Figure 1 provides an overview of the predictors that had relevant associations with basal forebrain volume or connectivity, separately for Aβ42/ptau positive and negative cases and central and peripheral inflammatory markers, yielding twelve different models. Relevant associations indicated that the 50% credibility interval of the respective parameter's posterior distribution excluded zero. The posterior distributions of the most salient parameters are shown in Figures 2 through 4, an overview over all parameters is shown in Supplementary Figure 5.

For **basal forebrain volume**, in the **Aβ42/ptau-positive cases** the elastic net identified a negative effect of age, a diagnosis of MCI or a diagnosis of AD and a positive effect of a

diagnosis of SCD (compared to a diagnosis of healthy control). **CSF levels** of YKL40, and Il18 were negatively, and **CSF levels** of AXL and MCP1 were positively associated with basal forebrain volume. The posterior distributions of the most salient parameters of the CSF model are shown in Figure 2a. For **serum levels** relevant positive effects were found for CRP, C3, Factor-H, and MIF, and relevant negative effects were found for C4, Il6, and IL18. The corresponding posterior distributions of the most salient parameters can be found in Figure 2b.

In the **Aβ42/ptau-negative cases** the elastic net identified ten **CSF** measures and eight **serum** measures that were positively or negatively associated with **basal forebrain volume**, among them CSF sTREM2, CSF FABP3, CSF YKL40, and CSF IL-6, as well as serum complement C3 and serum IL-6. Details of the posterior distributions of all salient parameters can be found in Figures 2c and 2d, in Supplementary Figure 5c and 5d for all parameters.

Results for **anterior basal forebrain connectivity** in the **Aβ42/ptau-positive cases** were sparser. Only four CSF markers and only one serum marker had relevant associations with anterior basal forebrain connectivity, among them CSF ApoE protein and serum Il-18 (Figures 3a and 3b), but also in the **Aβ42/ptau-negative cases** relevant associations with anterior basal forebrain connectivity were only few with four **CSF** and three **serum** markers (Figures 3c and 3d).

For **posterior basal forebrain connectivity**, in the **Aβ42/ptau-positive cases** we found relevant associations with six **CSF** and eight **serum** markers (Figures 4a and 4b). In the **Aβ42/ptau-negative cases** there were no relevant associations of **posterior basal forebrain connectivity** with **CSF** markers, but only with nine **serum** markers (Figures 4c and 4d).

Estimates of the strengths of the effects

To estimate the added value of the CSF/serum makers which were identified in the previous data-driven analyses, we determined how much the strength of correlations between predictors and volume/functional connectivity measures increased from only the demographic predictors (including age, sex, education years and diagnosis) to the demographic predictors plus the most salient CSF/serum markers. The markers contributing are those reported in Figure 1

An overview of the results can be found in Figure 5. Substantial increases of demographic correlations by the additional markers were only found for Aβ42/ptau-positive cases in three constellations: CSF markers and serum markers with basal forebrain volume as outcome, and serum markers with basal forebrain posterior connectivity as outcome (at least 75% probability that effects were higher with than without CSF markers, see supplementary Figure 6 for an example). In addition, CSF markers substantially contributed to prediction of posterior basal forebrain connectivity, however, the correlation with demographics alone was only $r < 0.20$, rendering the overall effect of little relevance. In all other constellations, CSF and serum markers contributed only modest effects.

Discussion

We investigated associations of inflammatory CSF and serum markers with volumes and functional connectivity of cholinergic basal forebrain in a group of older adults spanning the AD spectrum. Cases were stratified according to the CSF Aβ42/ptau ratio, indicating absence or presence of AD pathology.

Contrary to our *a priori* hypothesis which we had based on [12], we found evidence in favor of the absence of an effect of basal forebrain volumes and functional connectivity on CSF levels of sTREM2 and serum levels of complement C3, both in Aβ42/ptau ratio positive and negative cases. sTREM2 had been found involved in seeding of amyloid plaques [34], and increased with in vivo measures of microglia activation [35] in transgenic mouse models, suggesting a role in microglia-related phagocytosis of amyloid. Complement C3 as key factor in the complement cascade was found upregulated and associated with amyloid plaques containing dystrophic neurites in AD brains [36]. APP/PS1 mutation carrying mice with C3 knock-out demonstrated partly rescued cognitive phenotype and protection from neuron and synapse loss compared to APP/PS1 transgenic animals [37]. Peripheral and central cholinergic activity was found to be an endogenous factor to check innate immune response to different pathologies [9-11]. Our findings partly disagree with a previous study in preclinical AD cases [12]. This study had found that serum complement C3 at baseline was associated with a subsequently steeper decline of basal forebrain volume [12]. Based on sTREM2 and complement C3 alone we could not contribute convincing evidence from human data for the hypothesis that the cholinergic system modulated the microglia and complement-mediated response to Aβ and tau pathology. Of note, this conclusion is based on cross-sectional data only so that this does not preclude effects of baseline brain volume on longitudinal change in inflammatory markers. The higher power of longitudinal compared with cross-sectional

analyses has been shown before empirically using genetic and neuroimaging markers as trait and state markers of disease, respectively [38]. In addition, the group comparisons of basal forebrain volume followed a pattern that would indicate that higher volume reflects more preserved structural integrity within the AD spectrum. However, for functional connectivity evidence was in favour of no group effect, suggesting compensatory effects in early stages of AD and questioning its usefulness as a direct marker of basal forebrain functional integrity in the AD spectrum.

Beyond sTREM2 and C3, a previous study had found no direct association of CSF levels of YKL40 und MCP-1 as markers of microglial activation with voxel-based measures of white matter microstructural integrity from diffusion tensor imaging in cognitively healthy middle-aged to older people from the WRAP cohort [39]. This study reported, however, an interaction effect of MCP-1 with CSF Aβ42 on regionally restricted white matter regions in frontal and inferior temporal lobes [39]. A panel of anti- and pro-inflammatory serum markers was not associated with regional cortical and subcortical grey matter volumes in cognitively healthy older adults from the SNAC-K cohort [40]. Both studies did not include the basal forebrain as target region, and the study using a larger panel of markers [40] did not employ methods of variable selection.

In conclusion, preclinical data suggest an effect of cholinergic system integrity on the inflammatory response to danger-associated molecular patterns, but evidence from human studies, mostly focusing on a small number of selected inflammatory markers, is very limited so far. We would argue that a single inflammatory marker from CSF or serum or an unsystematic selection of markers from a larger panel may not be sufficient to capture the complex central and peripheral immune response to Aβ and ptau pathology. Therefore, we went beyond the previous studies and used a data driven approach to explore sets of

inflammatory markers from CSF and serum that may be associated with cholinergic system changes in Aβ/ptau positive and negative cases. We used penalized regression to avoid overfitting. We chose elastic net regularization as this penalty can handle groups of correlated variables within a larger number of variables ([32], page 56), a feature which also characterizes the current sets of CSF and serum markers (as shown in Figure 1 of [23]).

Subsequently, we will discuss the models where the inflammatory markers substantially contributed to the predictive value of the demographic characteristics (Figure 5). In the other models the size of the effect appeared small so that discussing the contributing markers may be premature lacking further confirmation.

For the basal forebrain volume in the Aβ/ptau positive cases, likelihood was at least 75% that the serum and CSF markers contributed to the model fit compared with the demographic predictors alone. As a side note, this analysis illustrates the beauty of the Bayesian approach to enable a direct estimate for the relative likelihood of the data under the null and the alternative hypothesis. CSF and serum levels of IL-18 were negatively associated with basal forebrain volume. IL-18 serum levels had been found increased in prodromal and clinical stages of AD in previous studies [41, 42], while an earlier study with very small sample size showed no effects [43]. Functionally, IL-18 is released as proinflammatory cytokine downstream of NLRP3 inflammasome activation [44] and part of a cascade inducing amyloid plaque formation [45, 46]. The negative association of basal forebrain volume and levels of IL-18 in CSF and serum would be consistent with an inhibiting effect of cholinergic stimulation on microglial response to Aβ and ptau pathology [47]. We want to point out again, however, that given the exploratory nature of this analysis, this is a pure post-hoc explanation. In concert with IL-18, CSF levels of YKL40 were negatively associated with basal forebrain volume in the Aβ/ptau positive cases. A previous study used voxel-based analysis of grey matter

volume changes over two years in cognitively healthy people. They found a significant positive association of YKL40 baseline CSF levels with a small inferior parietal cluster of change in grey matter volume over time [48]. YKL40 is expressed by reactive astrocytes [49] with elevated CSF levels in prodromal and early dementia stages of AD [50]. Our finding suggests lower levels of CSF YKL40 in presence of preserved cholinergic basal forebrain volume. In addition, in the Aβ/ptau positive cases, CSF levels of soluble Axl receptor tyrosine kinase (sAXL) and MCP-1 were positively associated with basal forebrain volume. MCP-1 is a chemokine attracting microglia to brain regions affected by pathology [51]. Co-expression of MCP-1 increased Aβ pathology in APP transgenic mice [52]. MCP-1 levels were increased in the CSF of AD patients in some [53], but not all [54, 55] previous studies. In MCI, MCP-1 levels in CSF were associated with faster cognitive decline [55]. Increase was mainly found at the dementia, but not the preclinical [53] or prodromal stages of AD [56]. Culture of microglia from the brains of AD patients compared with non-demented older people showed release of MCP-1 in response to Aβ peptide exposure which was, however, not different between AD and controls [57]. Together, these data suggest a potential disease accelerating role of MCP-1 starting at the prodromal and early clinical, but not the preclinical stages of AD. Therefore, the positive association of MCP-1 with basal forebrain volume in our Aβ/ptau positive cases is unexpected, since more preserved basal forebrain volume would indicate less affection by pathology.

Soluble AXL levels were associated with longitudinal decrease of CSF Aβ42 levels in cognitively healthy controls with normal Aβ42 levels at baseline, but not in healthy controls with abnormal Aβ42 at baseline and in AD patients [58]. These data may indicate that sAXL levels are increased in very early stages of AD pathogenesis, even preceding the onset of decreased Aβ42 levels in CSF and hence its parenchymal deposition. Therefore, our data may

indicate sAXL increase with more intact cholinergic basal forebrain volume in the presence of abnormal Aβ42/ptau levels in CSF.

For posterior basal forebrain connectivity in the Aβ42/ptau positive cases, likelihood was 96% that the serum markers contributed to the model fit compared with the demographic predictors alone. These markers included CRP, Ferritin, sAXL, complement C4, IP10, MIF, IL-18 and ApoE protein in serum. Posterior basal forebrain connectivity was found decreased in a regionally very restricted manner with higher global amyloid levels from amyloid sensitive PET measures in cognitively normal people with subjective memory decline [17]. In the current DELCODE cohort we had shown that pattern of basal forebrain connectivity was spatially consistent between diagnostic groups with small reductions in Aβ42 positive cases with subjective cognitive decline, MCI and AD dementia compared with controls [59]. Here, we found a positive association of posterior basal forebrain connectivity with proinflammatory markers, such as sAXL, complement C4 or IL-18, and inflammation markers such as CRP or Ferritin in serum. IP-10 is a downstream marker of Th1 cell response that was found unaltered in CSF and serum of MCI and AD dementia patients compared with controls [60-62]. CSF levels of Macrophage Migration Inhibitory Factor (MIF) were found only weakly associated with Aβ42, but more strongly with tau pathology [23], It is also considered an important opponent of glucocorticoid activity [63]. Its role in AD is unresolved with evidence for both pathogenetic as well as protective potential [64]. The basal forebrain posterior connectivity was positively associated with higher levels of proinflammatory and negatively with levels of potentially protective inflammatory markers in blood. This effect is consistent across markers. Functional connectivity may reflect a compensatory response to higher levels of inflammation. Of note, this is a post hoc interpretation that needs confirmation in an independent study.

Strengths of our study are the use of a comprehensive panel of CSF and serum markers of inflammatory response together with a systematic approach of feature selection using elastic net penalized regression. Bayesian analysis allowed us to directly assess levels of plausibility for the presence or the absence of an effect.

Limitations of our approach are the relatively small number of cases after stratification in Aβ42/ptau negative and positive cases that precluded us from analysing effects within diagnostic subgroups. Therefore, we used clinical diagnosis as a co-variate in our analyses. Cross-sectional data can only provide limited insight into the complex interplay of brain atrophy and peripheral and central inflammatory marker up- and down-regulation that may even follow a non-linear trajectory over time. Once available, we will use the longitudinal data of the DELCODE cohort to assess if basal forebrain volume is a predictor for the change in sTREM2 and complement C3 levels as well as of other neuroinflammatory markers over time across the AD spectrum. Of note, effect sizes for each single marker considered alone were small to moderate with direction of effects sometimes going in an unexpected direction. This may reflect the fact that each single marker is only a proxy for an underlying but unobservable mechanism of neuroinflammation. An alternative approach to make such a presumed unobservable mechanisms explicit would be the use of structural equation modelling where neuroinflammation would be treated as a latent variable. This factor cannot directly be measured but each marker level in CSF or serum would be considered a realization of a measurement related to this latent factor. This may help to generate more consistency of findings across different cohorts, however, at the cost of allowing only indirect inference on possibly underlying specific pathways of neuroinflammation. Finally, different approaches are available to determine functional connectivity of brain regions from fMRI data. Here, we used a method that we had established in two independent cohorts before [16, 17],

but we did not aim at exploring differences of results between different approaches of functional connectivity measurement.

In summary, with our cross-sectional data we could not confirm the assumption that sTREM2 and complement C3 release in response to Aβ42/ptau pathology would be moderated by volume or functional connectivity of the cholinergic basal forebrain. Data driven analysis across a large panel of CSF and serum markers of inflammatory response revealed several proinflammatory markers that were associated with basal forebrain volume and posterior connectivity in Aβ42/ptau positive cases. Due to the exploratory nature of this analyses, these data require independent confirmation. Together our findings provide preliminary evidence that cholinergic basal forebrain may be involved in the neuroinflammatory response to Aβ42 and ptau pathology in AD. The effect sizes, however, were small, suggesting that in vivo measures of neuroinflammatory markers in human studies may carry too much noise or may be of too little specificity to establish firm evidence for the role of cholinergic basal forebrain in the inflammatory response in AD.

Acknowledgements

The DELCODE study (Study-ID: BN012) was supported and conducted by the German Center for Neurodegenerative Diseases (DZNE). The data samples were provided by the DELCODE study group. Details and participating sites can be found at www.dzne.de/en/research/studies/clinical-studies/delcode. The DELCODE study was supported in respect to the MR imaging by Max Delbrück Center for Molecular Medicine in the Helmholtz Association (MDC), Berlin; Center for Cognitive Neuroscience Berlin (CCNB) at Freie Universität Berlin; Bernstein Center for Computational Neuroscience (BCCN), Berlin; Core Facility MR-Research in Neurosciences, University Medical Center Goettingen; Institute for Clinical Radiology, Ludwig Maximilian University, Munich; Institute of Diagnostic and Interventional Radiology, Pediatric Radiology and Neuroradiology, Rostock University Medical Center; and Magnetic Resonance research center, University Hospital Tuebingen.

Conflicts of interest/Competing interests

SJT participated in scientific advisory boards of Roche Pharma AG, Biogen, and MSD, and received lecture fees from Roche and MSD.

References:

[1] Kinney JW, Bemiller SM, Murtishaw AS, Leisgang AM, Salazar AM, Lamb BT (2018) Inflammation as a central mechanism in Alzheimer's disease. *Alzheimers Dement (N Y)* **4**, 575-590.

[2] Heneka MT, O'Banion MK (2007) Inflammatory processes in Alzheimer's disease. *J Neuroimmunol* **184**, 69-91.

[3] Ewers M, Franzmeier N, Suarez-Calvet M, Morenas-Rodriguez E, Caballero MAA, Kleinberger G, Piccio L, Cruchaga C, Deming Y, Dichgans M, Trojanowski JQ, Shaw LM, Weiner MW, Haass C, Alzheimer's Disease Neuroimaging I (2019) Increased soluble TREM2 in cerebrospinal fluid is associated with reduced cognitive and clinical decline in Alzheimer's disease. *Sci Transl Med* **11**.

[4] McGeer PL, McGeer EG (2013) The amyloid cascade-inflammatory hypothesis of Alzheimer disease: implications for therapy. *Acta Neuropathol* **126**, 479-497.

[5] Calsolaro V, Edison P (2016) Neuroinflammation in Alzheimer's disease: Current evidence and future directions. *Alzheimers Dement* **12**, 719-732.

[6] Cai Z, Hussain MD, Yan LJ (2014) Microglia, neuroinflammation, and beta-amyloid protein in Alzheimer's disease. *Int J Neurosci* **124**, 307-321.

[7] Heneka MT, O'Banion MK, Terwel D, Kummer MP (2010) Neuroinflammatory processes in Alzheimer's disease. *J Neural Transm (Vienna)* **117**, 919-947.

[8] Bartus RT, Dean RL, 3rd, Beer B, Lippa AS (1982) The cholinergic hypothesis of geriatric memory dysfunction. *Science* **217**, 408-414.

[9] Shytle RD, Mori T, Townsend K, Vendrame M, Sun N, Zeng J, Ehrhart J, Silver AA, Sanberg PR, Tan J (2004) Cholinergic modulation of microglial activation by alpha 7 nicotinic receptors. *J Neurochem* **89**, 337-343.

[10] Lehner KR, Silverman HA, Addorisio ME, Roy A, Al-Onaizi MA, Levine Y, Olofsson PS, Chavan SS, Gros R, Nathanson NM, Al-Abed Y, Metz CN, Prado VF, Prado MAM, Tracey KJ, Pavlov VA (2019) Forebrain Cholinergic Signaling Regulates Innate Immune Responses and Inflammation. *Front Immunol* **10**, 585.

[11] Yang Y, Peng Y, Yang J (2018) Galantamine protects against hydrochloric acid aspiration-induced acute respiratory distress syndrome in rabbits. *Tropical Journal of Pharmaceutical Research* **17**, 669-673.

[12] Schmitz TW, Soreq H, Poirier J, Spreng RN (2020) Longitudinal Basal Forebrain Degeneration Interacts with TREM2/C3 Biomarkers of Inflammation in Presymptomatic Alzheimer's Disease. *J Neurosci* **40**, 1931-1942.

[13] Jessen F, Spottke A, Boecker H, Brosseron F, Buerger K, Catak C, Fliessbach K, Franke C, Fuentes M, Heneka MT, Janowitz D, Kilimann I, Laske C, Menne F, Nestor P, Peters O, Priller J, Pross V, Ramirez A, Schneider A, Speck O, Spruth EJ, Teipel S, Vukovich R, Westerteicher C, Wiltfang J, Wolfsgruber S, Wagner M, Duzel E (2018) Design and first baseline data of the DZNE multicenter observational study on predementia Alzheimer's disease (DELCODE). *Alzheimers Res Ther* **10**, 15.

[14] Kilimann I, Grothe M, Heinsen H, Alho EJ, Grinberg L, Amaro E, Jr., Dos Santos GA, da Silva RE, Mitchell AJ, Frisoni GB, Bokde AL, Fellgiebel A, Filippi M, Hampel H, Kloppel S, Teipel SJ (2014) Subregional basal forebrain atrophy in Alzheimer's disease: a multicenter study. *J Alzheimers Dis* **40**, 687-700.

[15] Teipel SJ, Flatz WH, Heinsen H, Bokde AL, Schoenberg SO, Stockel S, Dietrich O, Reiser MF, Moller HJ, Hampel H (2005) Measurement of basal forebrain atrophy in Alzheimer's disease using MRI. *Brain* **128**, 2626-2644.

[16] Fritz HJ, Ray N, Dyrba M, Sorg C, Teipel S, Grothe MJ (2019) The corticotopic organization of the human basal forebrain as revealed by regionally selective functional connectivity profiles. *Hum Brain Mapp* **40**, 868-878.

[17] Chiesa PA, Cavedo E, Grothe MJ, Houot M, Teipel SJ, Potier MC, Habert MO, Lista S, Dubois B, Hampel H, Group IN-pS, the Alzheimer Precision Medicine I (2019) Relationship between Basal Forebrain Resting-State Functional Connectivity and Brain Amyloid-beta Deposition in Cognitively Intact Older Adults with Subjective Memory Complaints. *Radiology* **290**, 167-176.

[18] Zou H, Hastie T (2005) Regularization and variable selection via the elastic net. *Journal of the Royal Statistical Society Series B-Statistical Methodology* **67**, 301-320.

[19] Jessen F, Amariglio RE, van Boxtel M, Breteler M, Ceccaldi M, Chetelat G, Dubois B, Dufouil C, Ellis KA, van der Flier WM, Glodzik L, van Harten AC, de Leon MJ, McHugh P, Mielke MM, Molinuevo JL, Mosconi L, Osorio RS, Perrotin A, Petersen RC, Rabin LA, Rami L, Reisberg B, Rentz DM, Sachdev PS, de la Sayette V, Saykin AJ, Scheltens P, Shulman MB, Slavin MJ, Sperling RA, Stewart R, Uspenskaya O, Vellas B, Visser PJ, Wagner M, Subjective Cognitive Decline Initiative Working G (2014) A conceptual framework for research on subjective cognitive decline in preclinical Alzheimer's disease. *Alzheimers Dement* **10**, 844-852.

[20] Albert MS, DeKosky ST, Dickson D, Dubois B, Feldman HH, Fox NC, Gamst A, Holtzman DM, Jagust WJ, Petersen RC, Snyder PJ, Carrillo MC, Thies B, Phelps CH (2011) The diagnosis of mild cognitive impairment due to Alzheimer's disease: recommendations from the National Institute on Aging-Alzheimer's Association workgroups on diagnostic guidelines for Alzheimer's disease. *Alzheimers Dement* **7**, 270-279.

[21] McKhann GM, Knopman DS, Chertkow H, Hyman BT, Jack CR, Jr., Kawas CH, Klunk WE, Koroshetz WJ, Manly JJ, Mayeux R, Mohs RC, Morris JC, Rossor MN, Scheltens P, Carrillo MC, Thies B, Weintraub S, Phelps CH (2011) The diagnosis of dementia due to Alzheimer's disease: recommendations from the National Institute on Aging-Alzheimer's Association workgroups on diagnostic guidelines for Alzheimer's disease. *Alzheimers Dement* **7**, 263-269.

[22] Bertens D, Tijms BM, Scheltens P, Teunissen CE, Visser PJ (2017) Unbiased estimates of cerebrospinal fluid beta-amyloid 1-42 cutoffs in a large memory clinic population. *Alzheimers Res Ther* **9**, 8.

[23] Brosseron F, Kolbe CC, Santarelli F, Carvalho S, Antonell A, Castro-Gomez S, Tacik P, Namasivayam AA, Mangone G, Schneider R, Latz E, Wullner U, Svenningsson P, Sanchez-Valle R, Molinuevo JL, Corvol JC, Heneka MT, group As (2020) Multicenter Alzheimer's and Parkinson's disease immune biomarker verification study. *Alzheimers Dement* **16**, 292-304.

[24] Kurth F, Gaser C, Luders E (2015) A 12-step user guide for analyzing voxel-wise gray matter asymmetries in statistical parametric mapping (SPM). *Nat Protoc* **10**, 293-304.

[25] Chao-Gan Y, Yu-Feng Z (2010) DPARSF: A MATLAB Toolbox for "Pipeline" Data Analysis of Resting-State fMRI. *Front Syst Neurosci* **4**, 13.

[26] Franzmeier N, Caballero MAA, Taylor ANW, Simon-Vermot L, Buerger K, Ertl-Wagner B, Mueller C, Catak C, Janowitz D, Baykara E, Gesierich B, Duering M, Ewers M, Alzheimer's Disease Neuroimaging I (2017) Resting-state global functional connectivity as a biomarker of cognitive reserve in mild cognitive impairment. *Brain Imaging Behav* **11**, 368-382.

[27] Goodman S (2008) A dirty dozen: Twelve P-value misconceptions. *Seminars in Hematology* **45**, 135-140.

[28] Wagenmakers EJ, Marsman M, Jamil T, Ly A, Verhagen J, Love J, Selker R, Gronau QF, Smira M, Epskamp S, Matzke D, Rouder JN, Morey RD (2018) Bayesian inference for psychology. Part I: Theoretical advantages and practical ramifications. *Psychonomic Bulletin & Review* **25**, 35-57.

[29] Tibshirani R (1996) Regression shrinkage and selection via the Lasso. *Journal of the Royal Statistical Society Series B-Methodological* **58**, 267-288.

[30] Li Q, Lin N (2010) The Bayesian Elastic Net. *Bayesian Analysis* **5**, 151-170.

[31] van Erp S, Oberski DL, Mulder J (2019) Shrinkage priors for bayesian regularized regression. *J. Math. Psychol.* **89**, 31-50.

[32] Hastie T, Tibshirani R, Wainwright M (2015) *Statistical learning with sparsity: the Lasso and generalizations*, Chapman and Hall/CRC, Boca Raton, FL.

[33] Kruschke JK (2015) *Doing Bayesian Data Analysis - A Tutorial with R, JAGS, and Stan*, Elsevier, San Diego, CA.

[34] Parhizkar S, Arzberger T, Brendel M, Kleinberger G, Deussing M, Focke C, Nuscher B, Xiong M, Ghasemigharagoz A, Katzmarski N, Krasemann S, Lichtenthaler SF, Muller SA, Colombo A, Monasor LS, Tahirovic S, Herms J, Willem M, Pettkus N, Butovsky O, Bartenstein P, Edbauer D, Rominger A, Erturk A, Grathwohl SA, Neher JJ, Holtzman DM, Meyer-Luehmann M, Haass C (2019) Loss of TREM2 function increases amyloid seeding but reduces plaque-associated ApoE. *Nat Neurosci* **22**, 191-204.

[35] Brendel M, Kleinberger G, Probst F, Jaworska A, Overhoff F, Blume T, Albert NL, Carlsen J, Lindner S, Gildehaus FJ, Ozmen L, Suarez-Calvet M, Bartenstein P, Baumann K, Ewers M, Herms J, Haass C, Rominger A (2017) Increase of TREM2 during Aging of an Alzheimer's Disease Mouse Model Is Paralleled by Microglial Activation and Amyloidosis. *Front Aging Neurosci* **9**, 8.

[36] Eikelenboom P, Hack CE, Kamphorst W, Rozemuller JM (1992) Distribution pattern and functional state of complement proteins and alpha 1-antichymotrypsin in cerebral beta/A4 deposits in Alzheimer's disease. *Res Immunol* **143**, 617-620.

[37] Shi Q, Chowdhury S, Ma R, Le KX, Hong S, Caldarone BJ, Stevens B, Lemere CA (2017) Complement C3 deficiency protects against neurodegeneration in aged plaque-rich APP/PS1 mice. *Sci Transl Med* **9**.

[38] Xu Z, Shen X, Pan W, Alzheimer's Disease Neuroimaging I (2014) Longitudinal analysis is more powerful than cross-sectional analysis in detecting genetic association with neuroimaging phenotypes. *PLoS One* **9**, e102312.

[39] Melah KE, Lu SY, Hoscheidt SM, Alexander AL, Adluru N, Destiche DJ, Carlsson CM, Zetterberg H, Blennow K, Okonkwo OC, Gleason CE, Dowling NM, Bratzke LC, Rowley HA, Sager MA, Asthana S, Johnson SC, Bendlin BB (2016) Cerebrospinal Fluid Markers of Alzheimer's Disease Pathology and Microglial Activation are Associated with Altered White Matter Microstructure in Asymptomatic Adults at Risk for Alzheimer's Disease. *J Alzheimers Dis* **50**, 873-886.

[40] Papenberg G, Ferencz B, Mangialasche F, Mecocci P, Cecchetti R, Kalpouzos G, Fratiglioni L, Backman L (2016) Physical activity and inflammation: effects on gray-matter volume and cognitive decline in aging. *Hum Brain Mapp* **37**, 3462-3473.

[41] Schipke CG, Menne F, Rubow S, Sigle JP, Peters O, Grimmer T (2020) Value of a Panel of 6 Serum Biomarkers to Differentiate Between Healthy Controls and Mild Cognitive Impairment Due to Alzheimer Disease. *Alzheimer Dis Assoc Disord* **34**, 318-324.

[42] Malaguarnera L, Motta M, Di Rosa M, Anzaldi M, Malaguarnera M (2006) Interleukin-18 and transforming growth factor-beta 1 plasma levels in Alzheimer's disease and vascular dementia. *Neuropathology* **26**, 307-312.

[43] Lindberg C, Chromek M, Ahrengart L, Brauner A, Schultzberg M, Garlind A (2005) Soluble interleukin-1 receptor type II, IL-18 and caspase-1 in mild cognitive impairment and severe Alzheimer's disease. *Neurochem Int* **46**, 551-557.

[44] Heneka MT, McManus RM, Latz E (2018) Inflammasome signalling in brain function and neurodegenerative disease. *Nat Rev Neurosci* **19**, 610-621.

[45] Hanslik KL, Ulland TK (2020) The Role of Microglia and the Nlrp3 Inflammasome in Alzheimer's Disease. *Front Neurol* **11**, 570711.

[46] Yap JKY, Pickard BS, Chan EWL, Gan SY (2019) The Role of Neuronal NLRP1 Inflammasome in Alzheimer's Disease: Bringing Neurons into the Neuroinflammation Game. *Mol Neurobiol* **56**, 7741-7753.

[47] Ke P, Shao BZ, Xu ZQ, Chen XW, Wei W, Liu C (2017) Activating alpha7 nicotinic acetylcholine receptor inhibits NLRP3 inflammasome through regulation of beta-arrestin-1. *CNS Neurosci Ther* **23**, 875-884.

[48] Falcon C, Monte-Rubio GC, Grau-Rivera O, Suarez-Calvet M, Sanchez-Valle R, Rami L, Bosch B, Haass C, Gispert JD, Molinuevo JL (2019) CSF glial biomarkers YKL40 and sTREM2 are associated with longitudinal volume and diffusivity changes in cognitively unimpaired individuals. *Neuroimage Clin* **23**, 101801.

[49] Bonneh-Barkay D, Wang G, Starkey A, Hamilton RL, Wiley CA (2010) In vivo CHI3L1 (YKL-40) expression in astrocytes in acute and chronic neurological diseases. *J Neuroinflammation* **7**, 34.

[50] Craig-Schapiro R, Perrin RJ, Roe CM, Xiong C, Carter D, Cairns NJ, Mintun MA, Peskind ER, Li G, Galasko DR, Clark CM, Quinn JF, D'Angelo G, Malone JP, Townsend RR, Morris JC, Fagan AM, Holtzman DM (2010) YKL-40: a novel prognostic fluid biomarker for preclinical Alzheimer's disease. *Biol Psychiatry* **68**, 903-912.

[51] Yang G, Meng Y, Li W, Yong Y, Fan Z, Ding H, Wei Y, Luo J, Ke ZJ (2011) Neuronal MCP-1 mediates microglia recruitment and neurodegeneration induced by the mild impairment of oxidative metabolism. *Brain Pathol* **21**, 279-297.

[52] Yamamoto M, Horiba M, Buescher JL, Huang D, Gendelman HE, Ransohoff RM, Ikezu T (2005) Overexpression of monocyte chemotactic protein-1/CCL2 in beta-amyloid precursor protein transgenic mice show accelerated diffuse beta-amyloid deposition. *Am J Pathol* **166**, 1475-1485.

[53] Nordengen K, Kirsebom BE, Henjum K, Selnes P, Gisladottir B, Wettergreen M, Torsetnes SB, Grontvedt GR, Waterloo KK, Aarsland D, Nilsson LNG, Fladby T (2019) Glial activation and inflammation along the Alzheimer's disease continuum. *J Neuroinflammation* **16**, 46.

[54] Blasko I, Lederer W, Oberbauer H, Walch T, Kemmler G, Hinterhuber H, Marksteiner J, Humpel C (2006) Measurement of thirteen biological markers in CSF of patients with Alzheimer's disease and other dementias. *Dement Geriatr Cogn Disord* **21**, 9-15.

[55] Westin K, Buchhave P, Nielsen H, Minthon L, Janciauskiene S, Hansson O (2012) CCL2 is associated with a faster rate of cognitive decline during early stages of Alzheimer's disease. *PLoS One* **7**, e30525.

[56] Shen XN, Niu LD, Wang YJ, Cao XP, Liu Q, Tan L, Zhang C, Yu JT (2019) Inflammatory markers in Alzheimer's disease and mild cognitive impairment: a meta-analysis and systematic review of 170 studies. *J Neurol Neurosurg Psychiatry* **90**, 590-598.

[57] Lue LF, Rydel R, Brigham EF, Yang LB, Hampel H, Murphy GM, Jr., Brachova L, Yan SD, Walker DG, Shen Y, Rogers J (2001) Inflammatory repertoire of Alzheimer's disease and nondemented elderly microglia in vitro. *Glia* **35**, 72-79.

[58] Mattsson N, Insel P, Nosheny R, Zetterberg H, Trojanowski JQ, Shaw LM, Tosun D, Weiner M, Alzheimer's Disease Neuroimaging I (2013) CSF protein biomarkers predicting longitudinal reduction of CSF beta-amyloid42 in cognitively healthy elders. *Transl Psychiatry* **3**, e293.

[59] Herdick M, Dyrba M, Fritz HJ, Altenstein S, Ballarini T, Brosseron F, Buerger K, Can Cetindag A, Dechent P, Dobisch L, Duezel E, Ertl-Wagner B, Fliessbach K, Dawn Freiesleben S, Frommann I, Glanz W, Dylan Haynes J, Heneka MT, Janowitz D, Kilimann I, Laske C, Metzger CD, Munk MH, Peters O, Priller J, Roy N, Scheffler K, Schneider A, Spottke A, Jakob Spruth E, Tscheuschler M, Vukovich R, Wiltfang J, Jessen F, Teipel S, Grothe MJ (2020) Multimodal MRI analysis of basal forebrain structure and function across the Alzheimer's disease spectrum. *Neuroimage Clin* **28**, 102495.

[60] Galimberti D, Venturelli E, Fenoglio C, Lovati C, Guidi I, Scalabrini D, Mariani C, Bresolin N, Scarpini E (2007) IP-10 serum levels are not increased in mild cognitive impairment and Alzheimer's disease. *Eur J Neurol* **14**, e3-4.

[61] Elahi FM, Casaletto KB, La Joie R, Walters SM, Harvey D, Wolf A, Edwards L, Rivera-Contreras W, Karydas A, Cobigo Y, Rosen HJ, DeCarli C, Miller BL, Rabinovici GD, Kramer JH (2020) Plasma biomarkers of astrocytic and neuronal dysfunction in early- and late-onset Alzheimer's disease. *Alzheimers Dement* **16**, 681-695.

[62] Hu WT, Howell JC, Ozturk T, Gangishetti U, Kollhoff AL, Hatcher-Martin JM, Anderson AM, Tyor WR (2019) CSF Cytokines in Aging, Multiple Sclerosis, and Dementia. *Front Immunol* **10**, 480.

[63] Calandra T, Bucala R (2017) Macrophage Migration Inhibitory Factor (MIF): A Glucocorticoid Counter-Regulator within the Immune System. *Crit Rev Immunol* **37**, 359-370.

[64] Petralia MC, Battaglia G, Bruno V, Pennisi M, Mangano K, Lombardo SD, Fagone P, Cavalli E, Saraceno A, Nicoletti F, Basile MS (2020) The Role of Macrophage Migration Inhibitory Factor in Alzheimer's Disease: Conventionally Pathogenetic or Unconventionally Protective? *Molecules* **25**.

Table 1: Patient demographics

	HC (*n* = 70)	Relatives (n = 20)	SCD (*n* = 82)	MCI (*n* = 58)	AD (*n* = 31)
Sex (female/male) [1]	38/32	15/5	36/46	19/39	19/12
Age (mean, 95% CI) [years][2]	68.8 (67.6 - 69.9)	65.2 (63.4 - 67.1)	70.7 (69.5 – 72.0)	72.5 (71.0 - 73.9)	73.7 (71.6 - 75.8)
Education (mean, 95% CI) [years][3]	14.7 (14.0 - 15.4)	13.5 (12.3 - 14.7)	15.1 (14.4 - 15.8)	14.3 (13.5 - 15.2)	14.0 (13.0 - 15.1)
MMSE score (mean, 95% CI)[4]	29.5 (29.3 – 29.7)	29.0 (28.4 – 29.5)	29.2 (29.0 – 29.4)	28.0 (27.5 – 28.5)	24.0 (22.8 – 25.2)
Aβ42/ptau positive/negative	3/67	2/18	14/68	25/33	28/3

HC = Healthy Controls, SCD = Subjective Cognitive Decline, MCI = Mild Cognitive Impairment, AD = Alzheimer's Dementia, MMSE = Mini-Mental State Examination.

[1]Bayes factor in favor of a dependence between diagnosis and sex (BF_{10}) = 11.4; i.e., the dependency between sex and diagnosis is 11.4 times more likely than the independence of both factors.

[2]Bayes factor in favor of a group effect (BF_{10}) = $7.2 * 10^6$

[3]Bayes factor in favor of a group effect (BF_{10}) = 0.14; i.e., the absence of a group effect is 7 times more likely than the presence of such effect.

[4]Bayes factor in favor of a group effect (BF_{10}) = $3.7*10^{39}$

Figure legends

Figure 1: Predictors according to amyloid status and basal forebrain measures

For each of the twelve penalized regression models (Aβ42/ptau positive (_p) vs. negative (_n) * CSF vs. serum * basal forebrain volume vs. posterior basal forebrain connectivity vs. anterior basal forebrain connectivity) we depicted those markers that showed a relevant effect, i.e. the 50% credibility interval of the marker's posterior distribution excluded zero. Red markers had a negative, blue markers a positive association.

Figure 2: Posterior distribution of most salient CSF and serum parameters for basal forebrain volume

Posterior distributions of the parameters whose 50% CI excluded zero. The shaded area within the frequency distribution curve from the posteriors of each marker indicate the 50% CI, the blue vertical line indicates the mean.

Figures show the CSF predictors (Figure 2a) and the serum predictors (Figure 2b) for Aβ42/ptau positive cases as well as the CSF predictors (Figure 2c) and the serum predictors (Figure 2d) for Aβ42/ptau negative cases.

Figure 2b: Serum parameters in Aβ42/ptau positive cases

For legend see Figure 2a.

Figure 2c: CSF parameters in Aβ42/ptau negative cases

For legend see Figure 2a.

Figure 2d: Serum parameters in Aβ42/ptau negative cases

For legend see Figure 2a.

Figure 3: Posterior distribution of CSF or serum parameters for anterior basal forebrain connectivity

The posterior distributions of the parameters whose 50% CI excluded zero predicting anterior basal forebrain connectivity. The shaded area within the frequency distribution curve from the posteriors of each marker indicate the 50% CI, the blue vertical line indicates the mean.

Figures show the CSF predictors (Figure 3a) and the serum predictors (Figure 3b) for Aβ42/ptau positive cases as well as the CSF predictors (Figure 3c) and the serum predictors (Figure 3d) for Aβ42/ptau negative cases.

Figure 4: Posterior distribution of CSF or serum parameters for posterior basal forebrain connectivity

The posterior distributions of the parameters whose 50% CI excluded zero predicting posterior basal forebrain connectivity. The shaded area within the frequency distribution curve from the posteriors of each marker indicate the 50% CI, the blue vertical line indicates the mean.

Figures show the CSF predictors (Figure 4a) and the serum predictors (Figure 4b) for Aβ42/ptau positive cases as well as the CSF predictors (Figure 4c) and the serum predictors (Figure 4d) for Aβ42/ptau negative cases.

Figure 5: Correlations between volumes and demographic vs. demographics plus salient CSF/serum parameters and probability of superiority

For each of the twelve penalized regression models (Aβ42/ptau positive vs. negative * CSF vs. serum * basal forebrain volume vs. posterior basal forebrain connectivity vs. anterior basal forebrain connectivity) we depicted the correlation for only the demographic predictors (red bars), the correlations for the demographic predictors plus the CSF/serum parameters (green bars) as well as the likelihood (in percent) that the correlation coefficient was higher with the CSF/serum parameters than with the demographic predictors alone (blue bars).

Figure 1: Predictors according to amyloid status and basal forebrain measures

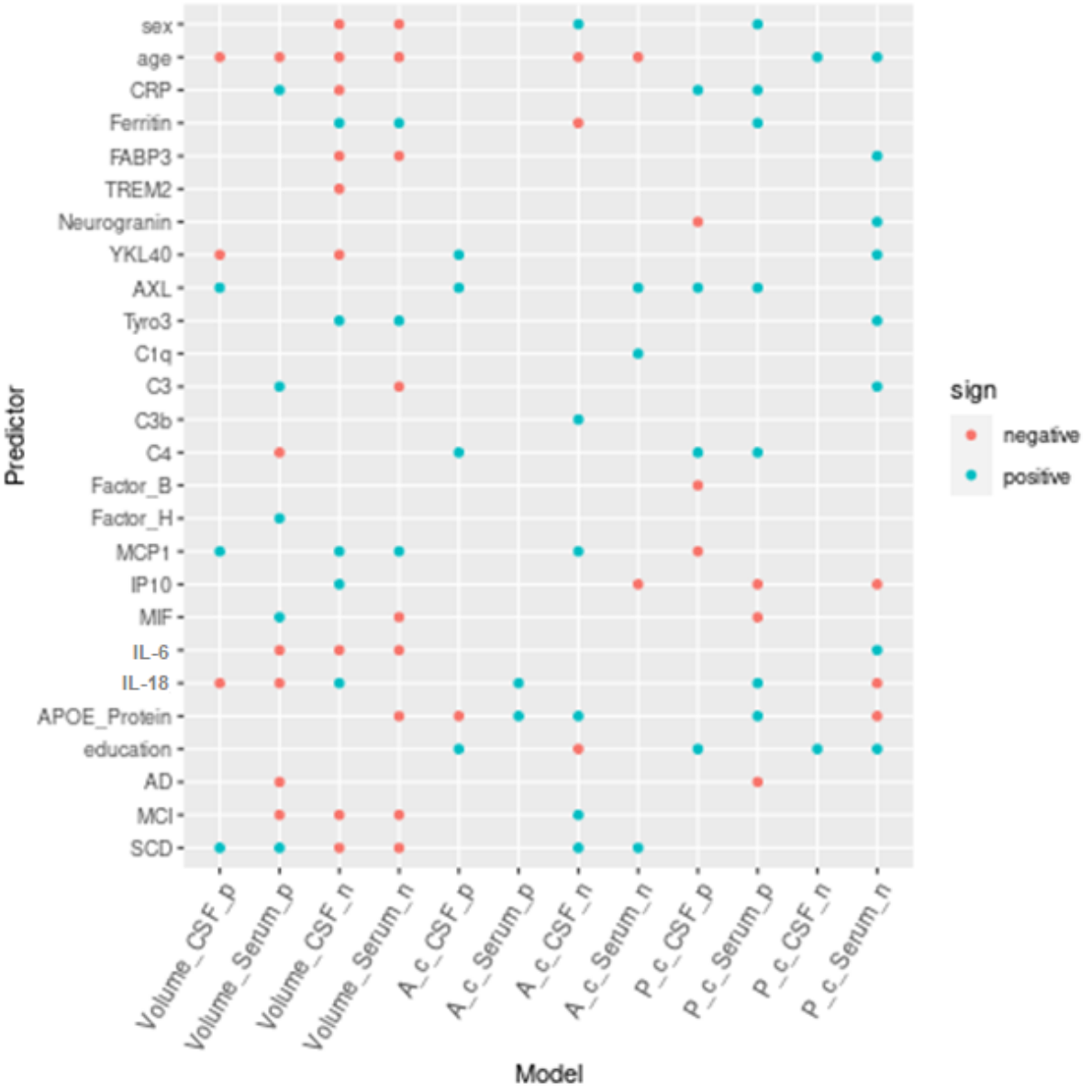

Figure 2: Posterior distribution of most salient CSF and serum parameters for basal forebrain volume

Figure 2a: Salient CSF and demographic parameters in Aβ42/ptau positive cases

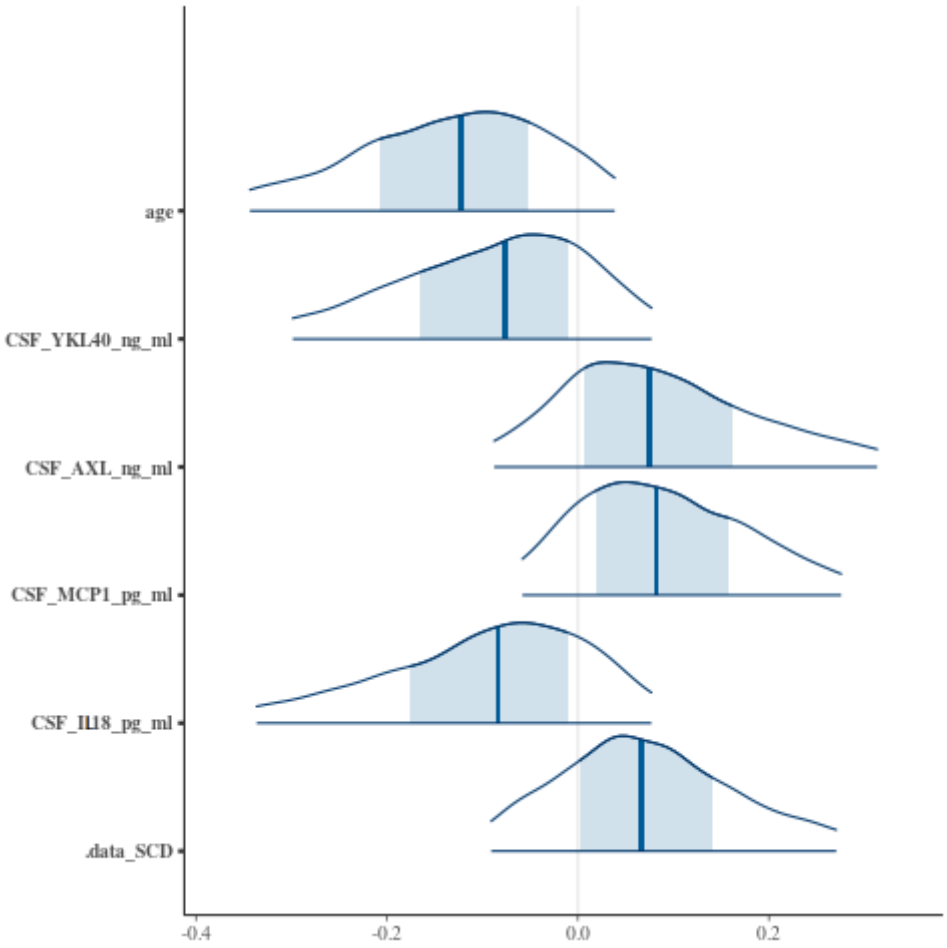

Figure 2b: Salient serum and demographic parameters in Aβ42/ptau positive cases

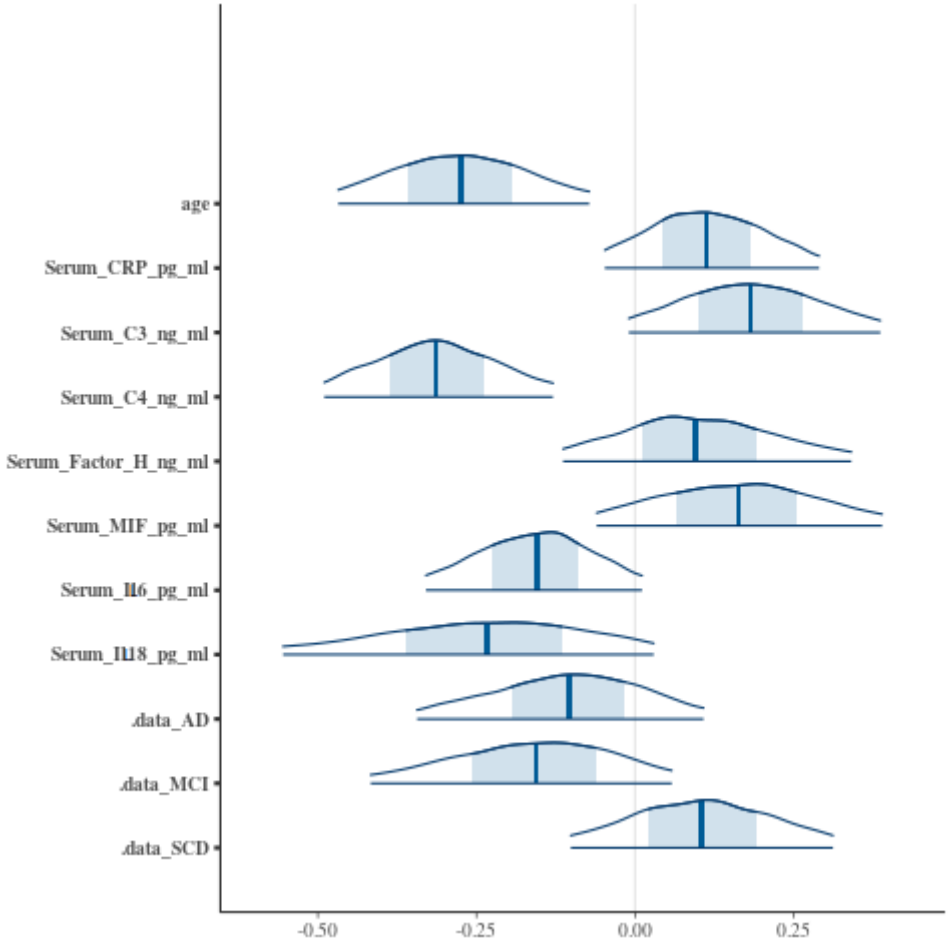

Figure 2c: Salient CSF and demographic parameters in Aβ42/ptau negative cases

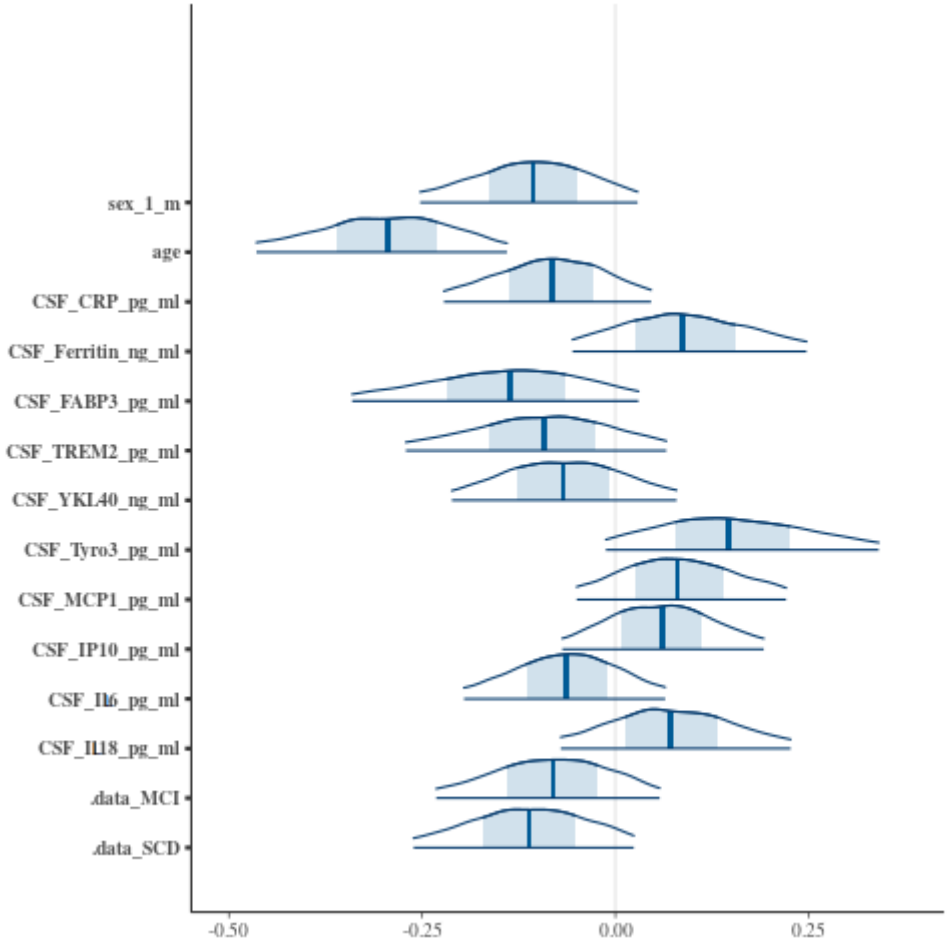

Figure 2d: Salient serum and demographic parameters in Aβ42/ptau negative cases

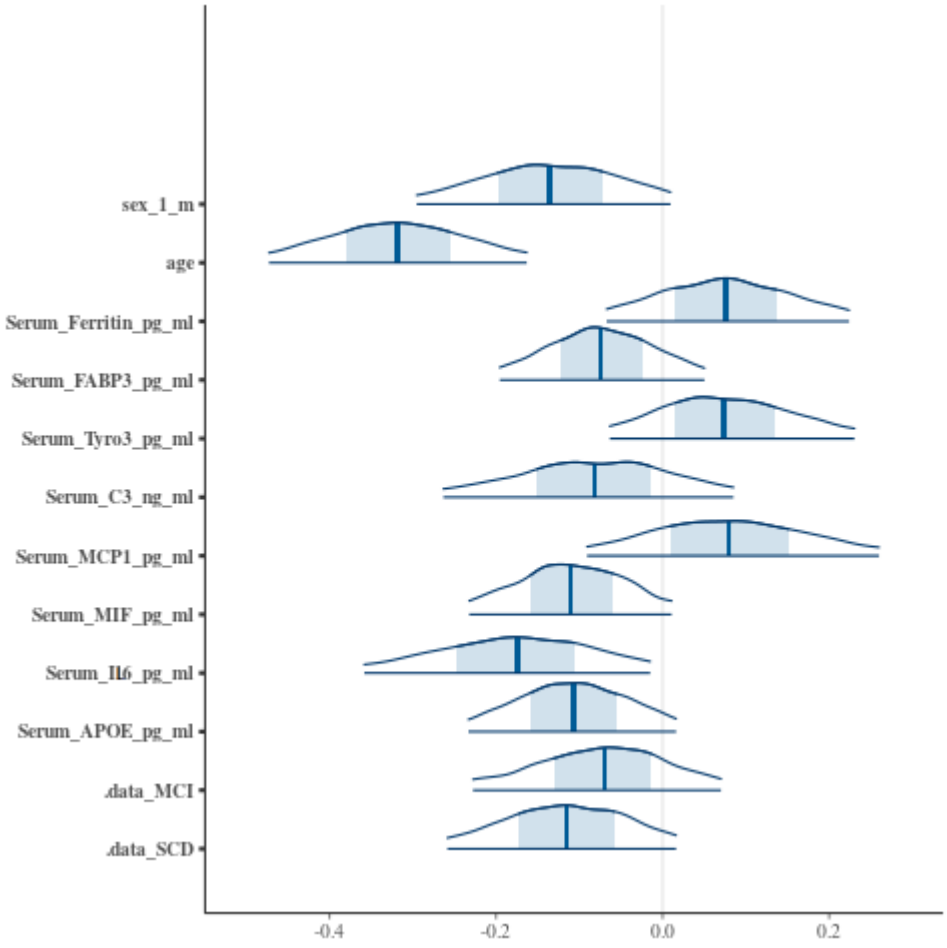

Figure 3: Posterior distribution of CSF or serum parameters for anterior basal forebrain connectivity

Figure 3a: Salient CSF and demographic parameters in Aβ42/ptau positive cases

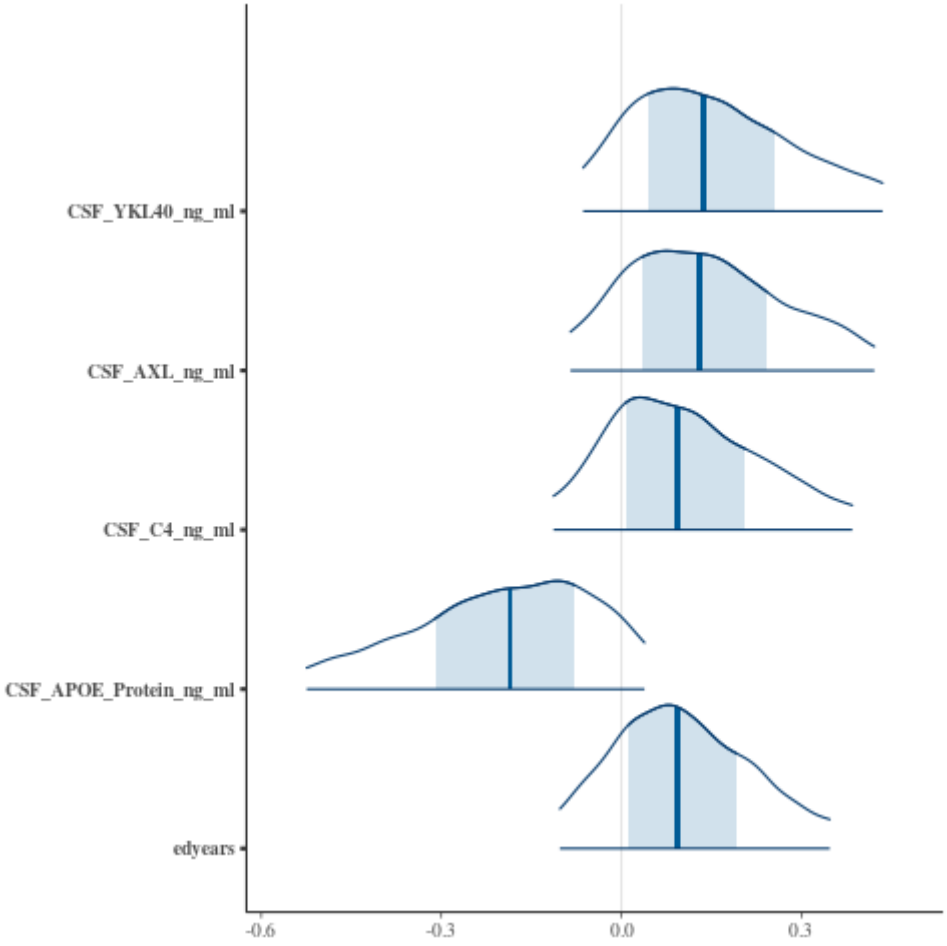

Figure 3b: Salient serum parameters in Aβ42/ptau positive cases

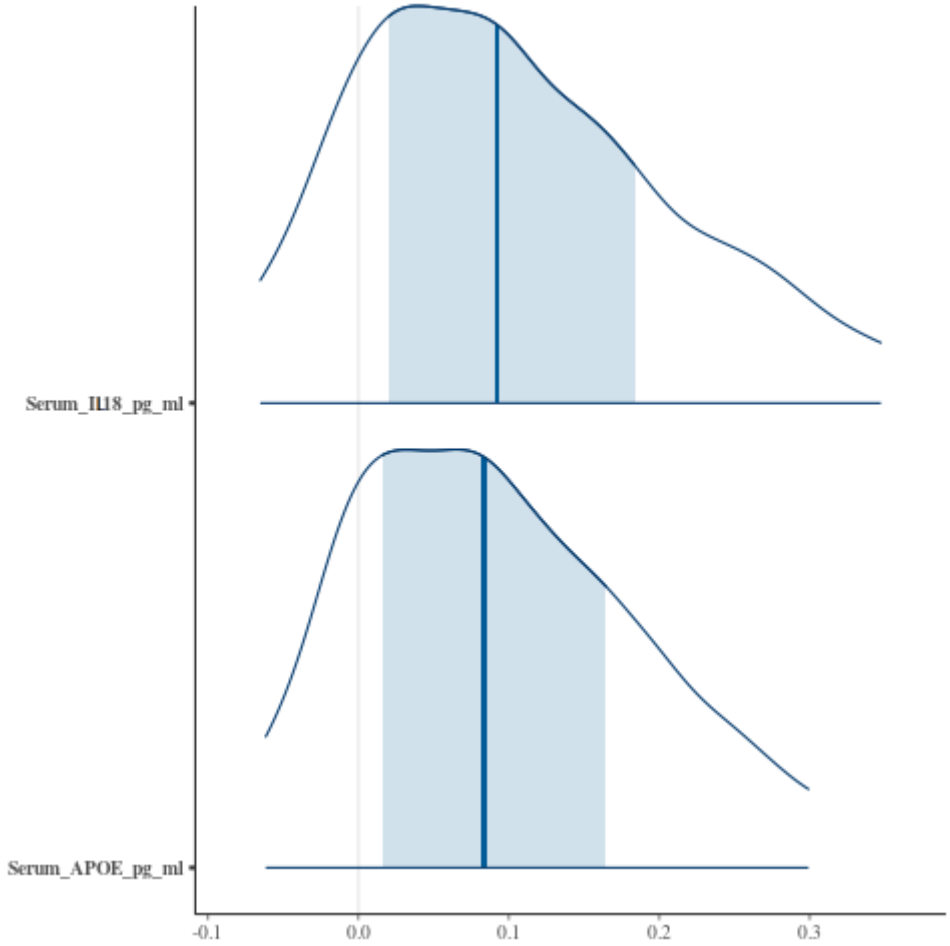

Figure 3c: Salient CSF and demographic parameters in Aβ42/ptau negative cases

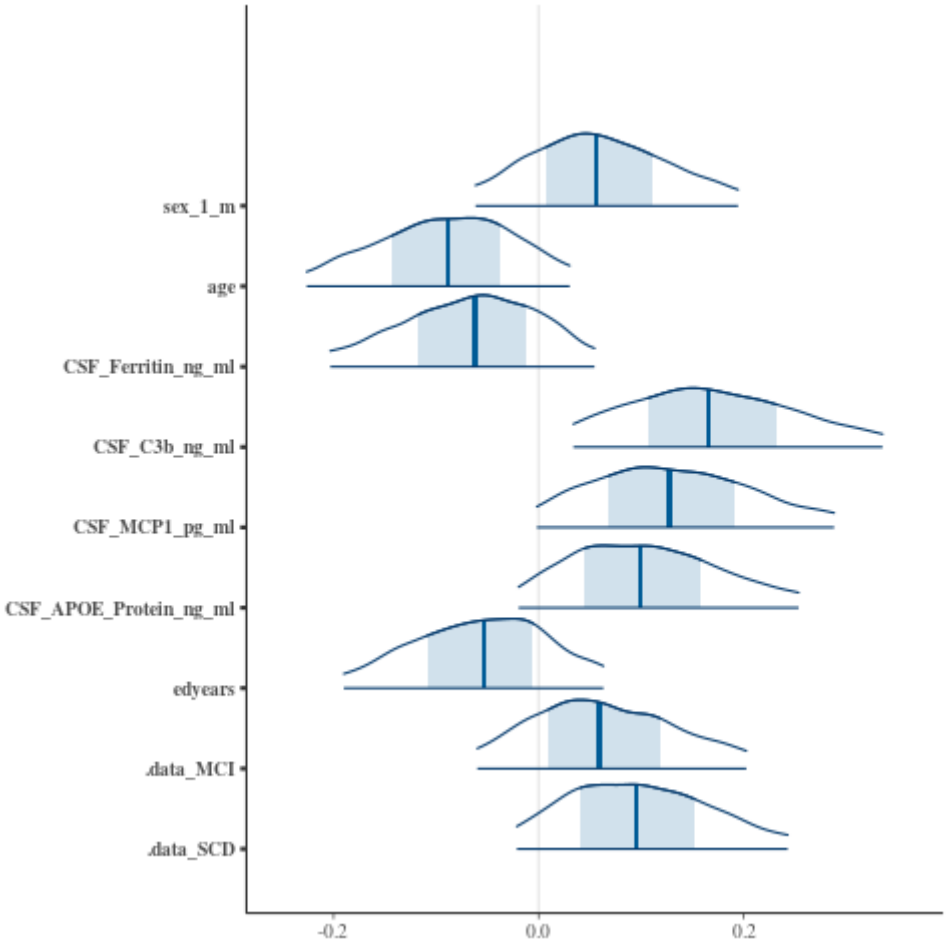

Figure 3d: Salient serum and demographic parameters in Aβ42/ptau negative cases

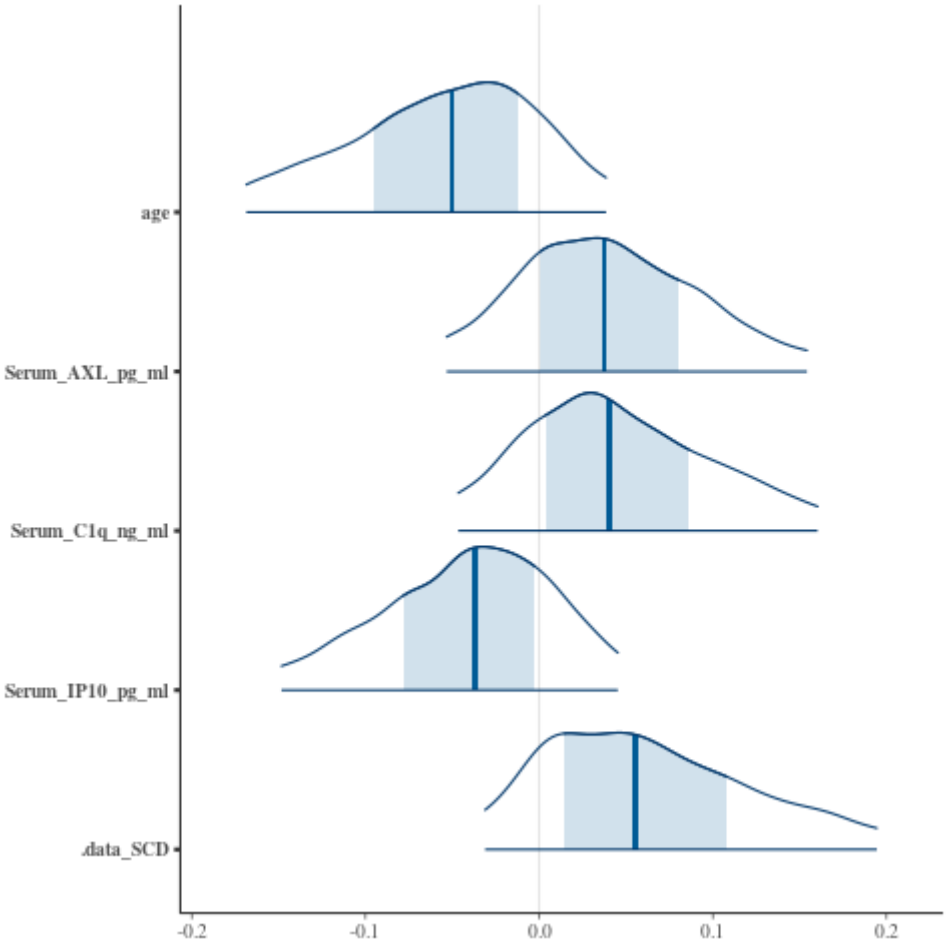

Figure 4: Posterior distribution of CSF or serum parameters for posterior basal forebrain connectivity

Figure 4a: Salient CSF and demographic parameters in Aβ42/ptau positive cases

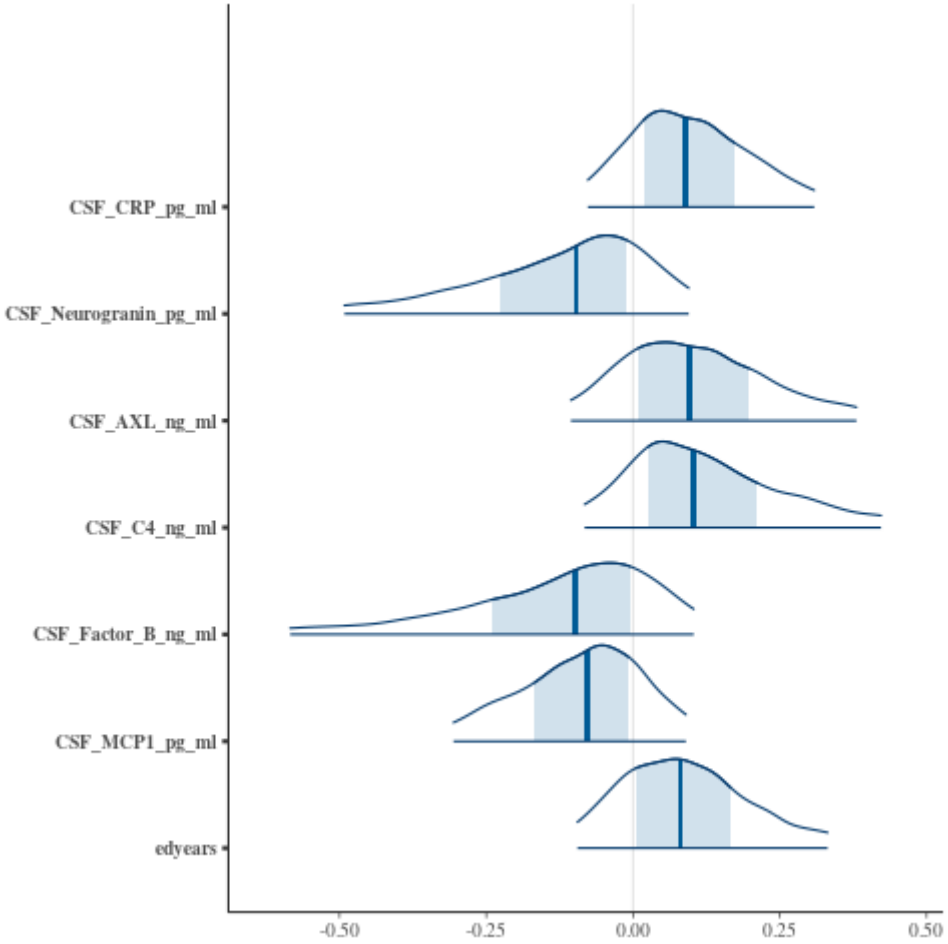

Figure 4b: Salient serum and demographic parameters in Aβ42/ptau positive cases

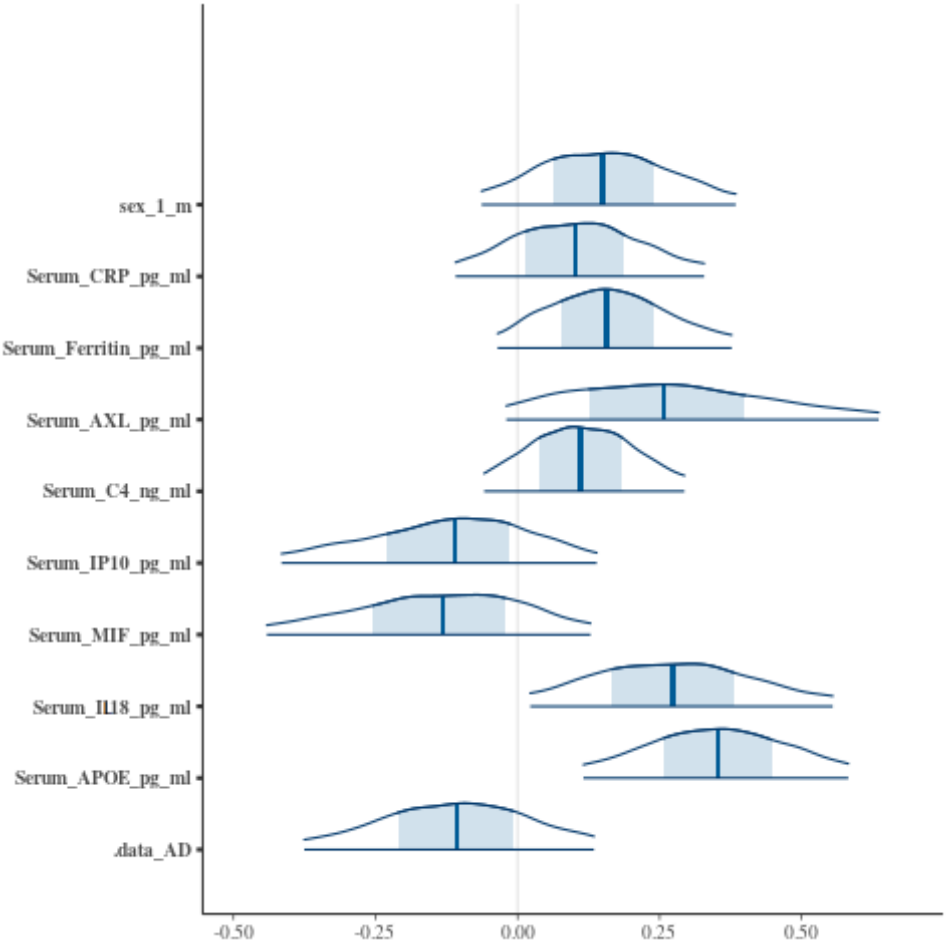

Figure 4c: Salient CSF and demographic parameters in Aβ42/ptau negative cases

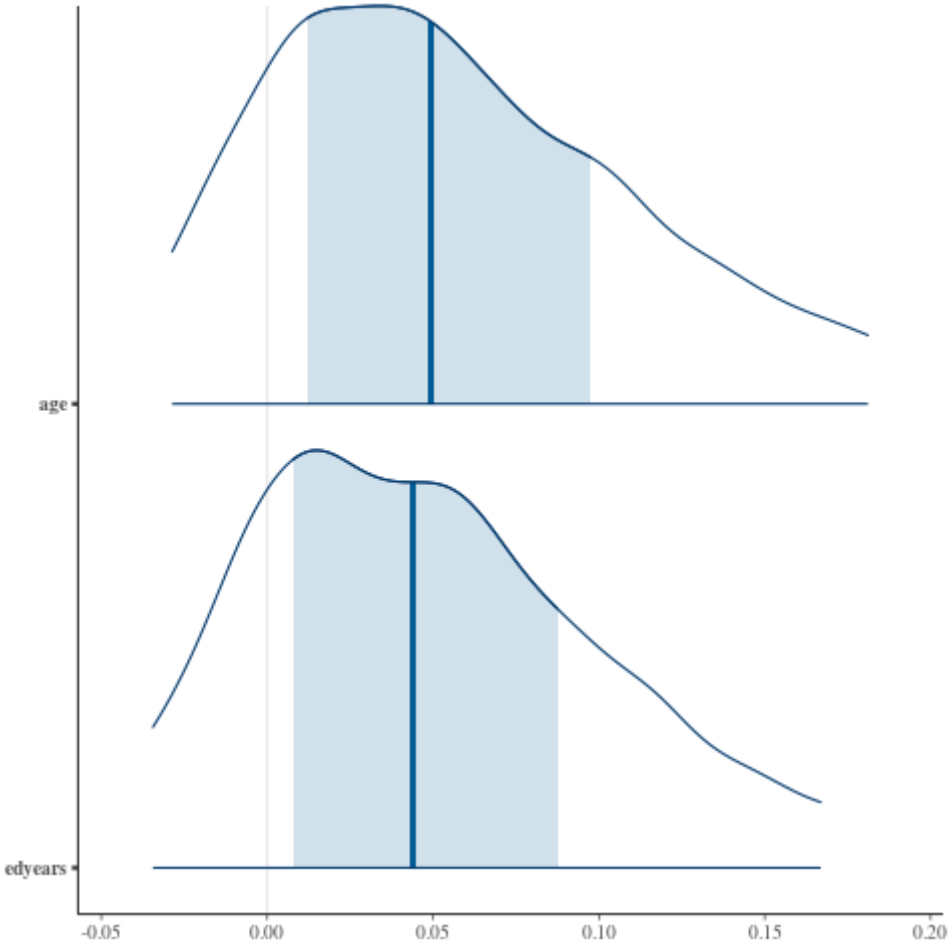

Figure 4d: Salient serum and demographic parameters in Aβ42/ptau negative cases

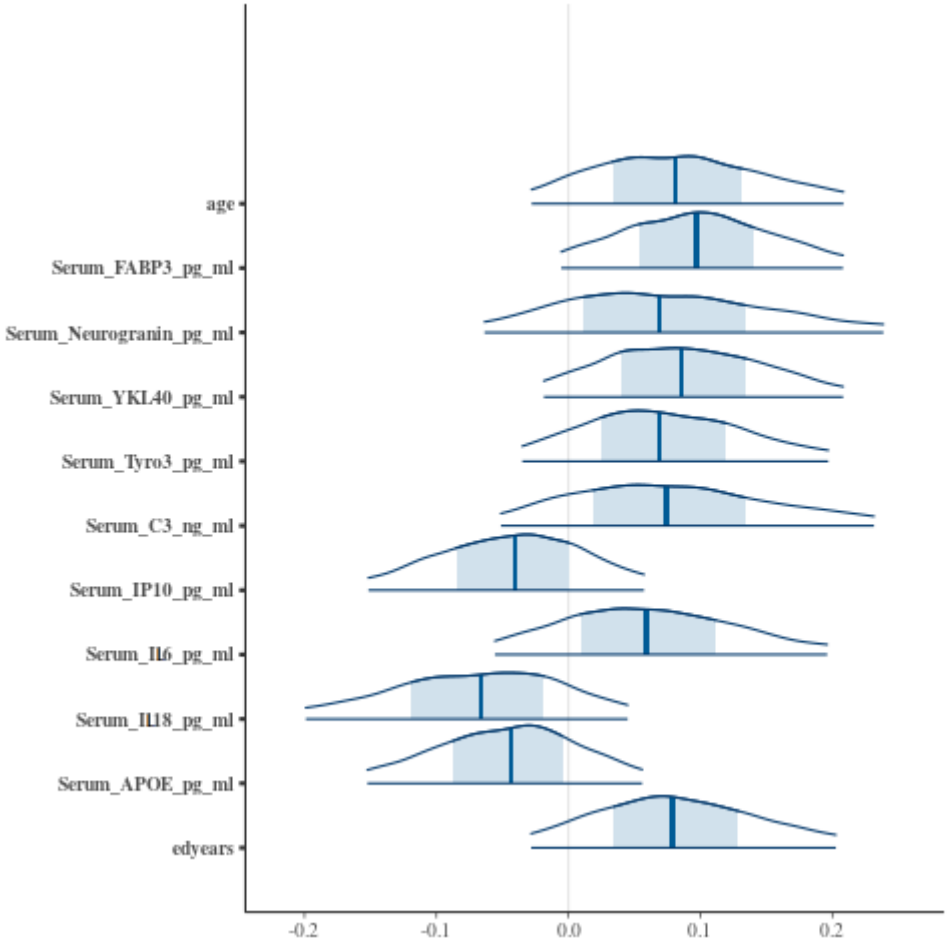

Figure 5: Correlations between volumes and demographic vs. demographics plus salient CSF/serum parameters and probability of superiority